A WAY OF PATTERN ANALYSIS OF TURBULENT STRUCTURE OF LOW-FREQUENCY EDDY-GROUP IN A CIRCULAR PIPE FLOW

KOHEI OGAWA, CHIAKI KURODA AND SHIRO YOSHIKAWA
Department of Chemical Engineering, Tokyo Institute of Technology, Tokyo 152

Key Words: Fluid Mechanics, Turbulent Flow, Circular Pipe, Eddy Group, Pattern Analysis, Radial Space Scale, Contour Line Map

Turbulent axial velocity fluctuations at sixteen radial positions in a circular pipe are measured simultaneously, and contour line maps of the velocity are drawn in time-radial position coordinates. On the basis of these maps, the change in velocity radial distribution with time is regarded as a pattern, and the time- and space-scales of the lower-frequency eddy-group which is predicted to influence the diffusion of fluid element are discussed. By a statistical method based on pattern analysis, the radial distribution of averaged space-scales of eddies is obtained. Additionally, smaller eddies which cannot be found by the statistical method are extracted through direct reading from the contour line maps, and the usefulness of regarding the turbulent flow field as a pattern is made clear.

Introduction

Transport phenomena and chemical reactions in chemical equipment depend greatly upon the flow condition. Particularly, the structure of turbulent flow is one of the important factors that control the capacity of the equipment.

It has been considered that the velocity fluctuation in a turbulent flow field consists of various frequencies, and energy spectra have been used to express the structure. In the previous paper,[4] a formula for the one-dimensional energy spectrum function for wide wavenumber ranges was proposed under the assumption that the turbulent flow field consists of eddy-groups, and it can be predicted that the space-scale of the lower-frequency eddy-group, which has many effects on the diffusion of fluid element, is large.

In the case of turbulent flow in a circular pipe, which is a representative item of equipment, the velocity has been measured independently at each radial position, and the characteristics of the turbulent flow are analyzed according to the measured velocity. But in the lower-frequency eddy-group, which is estimated to have a large space-scale, the velocity at each radial position doesn't fluctuate independently of one another and the movement of the eddy-group will have an influence upon the transport phenomena in the flow field. Therefore, simultaneous measurements of velocities at each radial position are indispensable in order to investigate the scale of the lower-frequency eddy-groups. However, simultaneous measurement has hardly been done even in the pipe flow of Newtonian fluids.

Received June 19, 1986. Correspondence concerning this article should be addressed to K. Ogawa.

The purpose of the present study is to gain information about the scale of the lower-frequency eddy-group in turbulent pipe flow from the viewpoint of pattern analysis. For that purpose, the velocity fluctuations at sixteen radial positions were measured simultaneously and contour line maps concerning the velocity were drawn in the two-dimensional space consisting of time and radial position. By making use of these maps, the shapes and the scales of eddies which correspond to the lower-frequency eddy-group will be discussed.

1. Experiments

The experimental apparatus is illustrated schematically in **Fig. 1**. The electrolyte solution as the test liquid in a reservoir tank is fed into an overflow tank with a pump. It flows down through the test pipe connected to the bottom of the overflow tank and returns to the reservoir tank. The overflow water from the overflow tank flows back to the reservoir tank directly. The test pipe, made of acrylic resin (69.7 mm inner diameter and 8.1 m total length) is set vertically. The velocity-measuring probe is set at a distance 7.5 m downstream from the inlet of the test pipe.

The rate of flow is regulated by a needle valve connected to the test pipe downstream of the test section.

An electrochemical probe which consists of sixteen platinum spheres (0.5 mm diameter and 2.18 mm = $0.063R$ interval between adjacent spheres) on an acrylic resin plate as shown in **Fig. 2** was used to measure the velocity fluctuations at sixteen radial positions simultaneously. It was already confirmed[2,3] that the axial velocity fluctuations could be measured by using these platinum sphere electrodes.

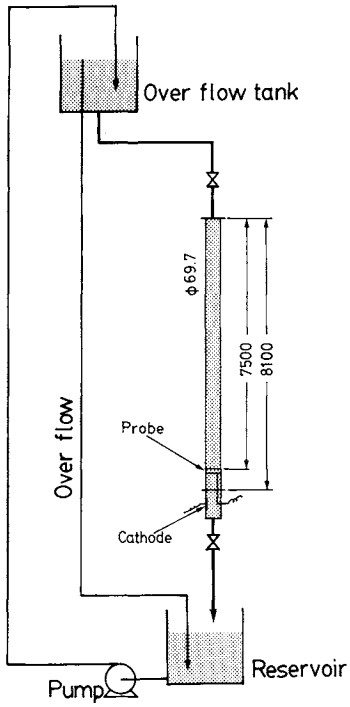

Fig. 1. Experimental apparatus.

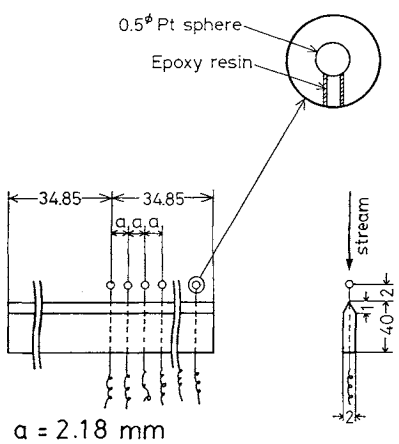

Fig. 2. Velocity-measuring probe.

Output of the probe was recorded on magnetic tapes at sampling intervals of 0.005 s (=200 Hz) by a multi-channel digital data recorder, and these data were analyzed by a computer. The sampling interval of 0.005 s was determined after confirmation[5] that the order of the average frequency of the lower-frequency eddy-group is the range of 1–5 Hz for the turbulent flow in the test pipe.

The experiments were carried out in the range of Reynolds numbers from 5900 to 21000, which corresponds to the region from undeveloped to fully developed turbulent flow.

2. Experimental Results

In the following, all contour line maps will be shown in coordinates of r/R and t because the original data were obtained by an Eulerian method.

2.1 Change in velocity distribution with time

Figure 3 shows an example of the change in axial velocity distribution with time at a Reynolds number of 17200 in the three-dimensional space consisting of dimensionless radial position (r/R), time (t) and axial velocity (U). In this figure, measured data are connected by straight lines to express velocity fluctuations which have larger scales than the intervals of adjacent measuring positions clearly. The simultaneous behavior of liquid elements at a few sequential radial positions can be observed in some regions, and these regions are predicted to be occupied by the lower-frequency eddy-group.

2.2 Contour line map of velocity

To express the lower-frequency eddy-groups clearly, contour line maps of velocity were drawn. **Figure 4**(a) and (b) are examples of these contour line maps. Abscissa and ordinate are dimensionless radial position and time, respectively. Each of these maps is drawn by using 65 velocity distribution data which are sampled at intervals of 0.1 s (=10 Hz). These maps are drawn by a least square method, which has been confirmed to be normal by comparing axial mean velocity profiles estimated from the contour line maps with universal ones. The regions between adjacent radial measuring positions are drawn by interpolation, so the contour lines of the velocity in such interpolated regions, particularly the regions near the pipe wall, may not be expressed completely. Accordingly, attention is paid to an eddy which extends over more than two radial measuring positions, so the shape of the contour lines in these regions have little influence on the analysis in this paper. The contour lines are drawn at intervals of 1.0 cm/s and each numerical value in these figure expresses the velocity of each line. In these maps, regions where the contour lines are extended in the radial direction can be observed, and it can be said that the liquid elements in these regions behave simultaneously. These regions are predicted to be occupied by the lower-frequency eddy-groups. And from these maps, it becomes clear that the frequency of fluctuation increases with increasing Reynolds number. In the following sections, these maps are regarded as turbulent flow patterns.

3. Analysis of the Turbulent Flow Patterns

3.1 Statistical method

First, the turbulent flow patterns are analyzed statistically according to an old method.

The contour line maps are treated as two-dimensional geometrical patterns. The data are arranged as shown in **Fig. 5** where abscissa and ordinate are dimensionless radial position and time, respectively, and the dots express the places where the data

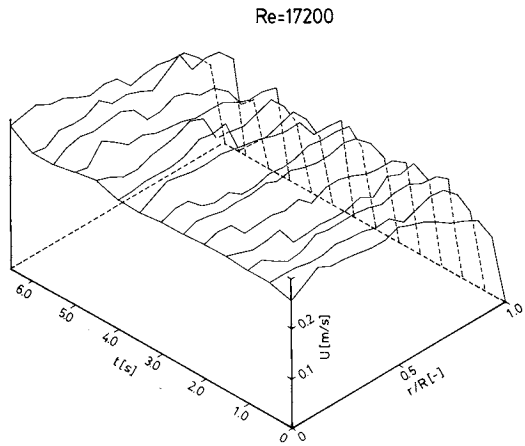

Fig. 3. Change in axial velocity distribution with time.

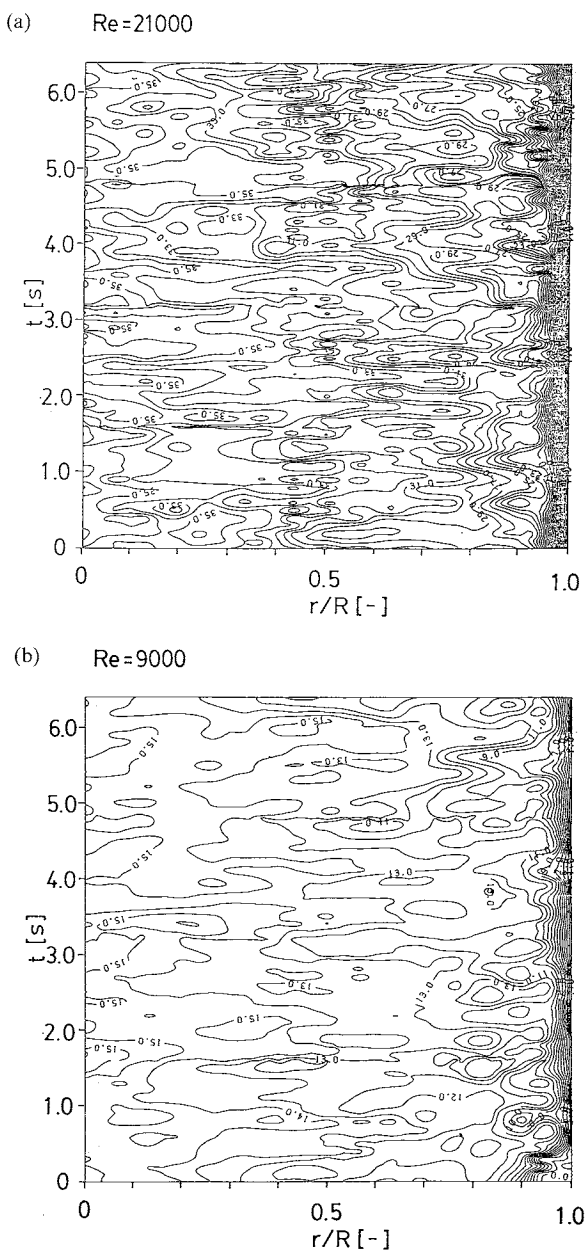

Fig. 4. Contour line map of velocity. (a) $Re=21000$; (b) $Re=9000$.

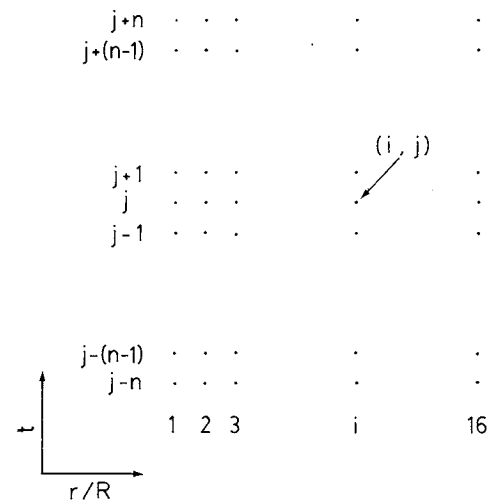

Fig. 5. Arrangement of data in the contour line map.

exist. The velocity at the point of radial position-i and time-j is designated $U(i,j)$ and the fluctuating part at $U(i,j)$ is defined as

$$u(i,j)=U(i,j)-\bar{U}(i) \tag{1}$$

where $\bar{U}(i)$ is the local mean velocity at radial position-i. To analyze the contour line maps quantitatively, the data which compose the maps are expanded into one-dimensional sequential data which are then arranged in order of time as follows:

$$\begin{aligned} &u(1,j-n),\ u(2,j-n),\ \cdots,\ u(i,j-n)\ ,\ \cdots \\ &,u(16,j-n),\ u(1,j-(n-1)),\ \cdots,\ u(i,j-(n-1))\ ,\cdots \\ &,u(1,j-1),\ \cdots,\ u(16,j-1),\ u(1,j),\ u(2,j)\ ,\ \cdots \\ &,u(16,j),\ u(1,j+1),\ \cdots,\ u(16,j+1),\ u(1,j+2)\ ,\cdots \end{aligned} \tag{2}$$

where n is an arbitrary integer.

Using this arrangement, the data can be analyzed statistically without consideration of the time and position, and the datum at every 16th data point is for the same radial position. Considering that there is a distance of 1/16 between two adjacent data, the distance between the noticed datum $u(i,j)$ and an arbitrary datum $u(m,j+n)$ can be shown as

$$d=(m-i)/16+n \tag{3}$$

Therefore, when $u(i,j)$ is set at $u(0)$, $u(m,j+n)$ can be written as $u(d)$. The correlation coefficient between $u(0)$ and $u(d)$ is defined as the following function of d:

$$C_i=\frac{\overline{u(0)u(d)}}{u_i'^2} \tag{4}$$

where u_i' is the intensity of velocity fluctuation at radial position-i.

This correlation coefficient can be obtained as an ensemble mean of 1848 arrangements of data. **Figure 6**(a), (b), (c) and (d) show some examples of the

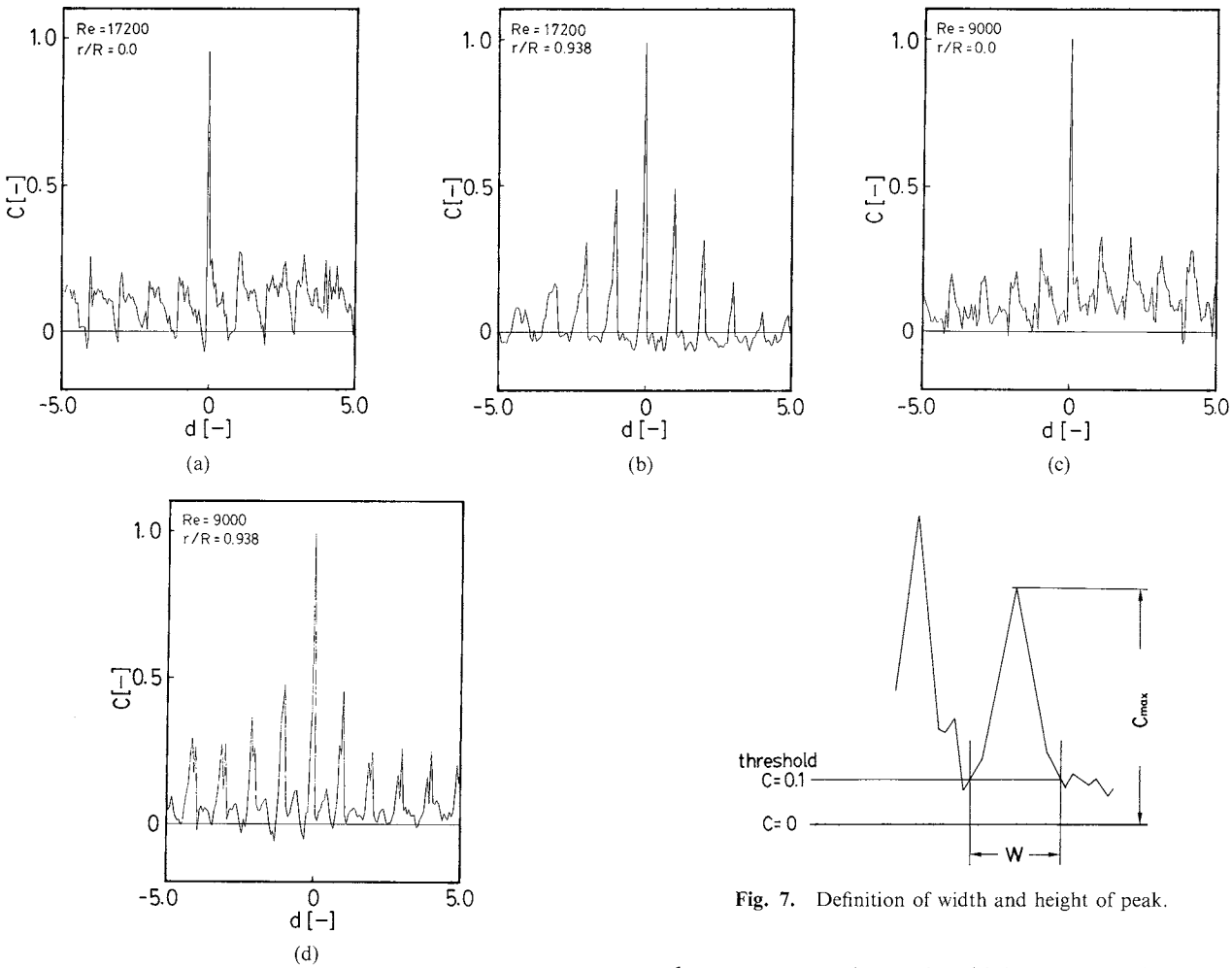

Fig. 6. Correlation curve. (a) $Re=17200$, $r/R=0.0$; (b) $Re=17200$, $r/R=0.938$; (c) $Re=9000$, $r/R=0.0$; (d) $Re=9000$, $r/R=0.938$.

Fig. 7. Definition of width and height of peak.

correlation curves according to the way of thinking described above. In some of them, some peaks appear periodically, and the height of the peaks decrease with increase of absolute value of d. The period of the appearance of the peak is about 1.0, and the periodicity shows that structures which are due to the lower-frequency eddy-groups exist near the noticed radial position. Additionally, the decrease in height of the peaks reveals the decay of the structures with increase of absolute value of d. On the other hand, in Fig. 6(a), the peak under the condition of $Re=17200$ at $r/R=0.0$ does not seem to be periodical. This shows that a structure which is due to the lower-frequency eddy-groups decays more rapidly than the sampling interval in the higher Reynolds number ranges. Additionally, it can be said that the periodicity of the peaks near the pipe wall is clearer than that near the center of the pipe.

Figure 7 shows a typical part of the correlation curve. Width (W) and height (C_{max}) of the peak are defined by using an appropriate threshold of $C=0.1$ as shown in this figure. The width of the peak seems to be a representative scale which corresponds to the radial space-scale of the lower-frequency eddy-group, and the height of the peak will show the degree of correlation between two points. These values, i.e. W and C_{max}, are measured for all peaks in each objective correlation curve and the average of all W values, $\bar{W}$, and the summation of all C_{max} values, ΣC_{max}, are calculated.

1) $\bar{W}$ Though it is very difficult to classify the operational conditions into low-Re group and high-Re group. $Re=10000$ is taken as the representative threshold value as a trial. By using the threshold, the operational conditions are divided into two Reynolds number groups. The average values of $\bar{W}$ at each radial position is calculated, and the results are shown in **Fig. 8**. There is no difference in the shape of the distribution for the low Reynolds number group from that for the high Reynolds number group. $\bar{W}$ takes maximum value at $r/R=0.5$, and approaches zero at $r/R=1$. This result predicts that the pipe wall disturbs the appearance of the lower-frequency eddy-groups. On the other hand, it seems that the shape of the distribution of $\bar{W}$ resembles that of eddy diffusivity which is reported by Hinze[1], though the dimensions of the two quantities are different from each other. This result may suggest that the radial space-scale of

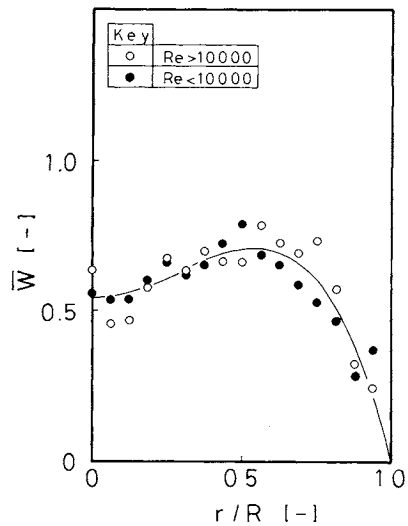

Fig. 8. Radial distribution of $\bar{W}$.

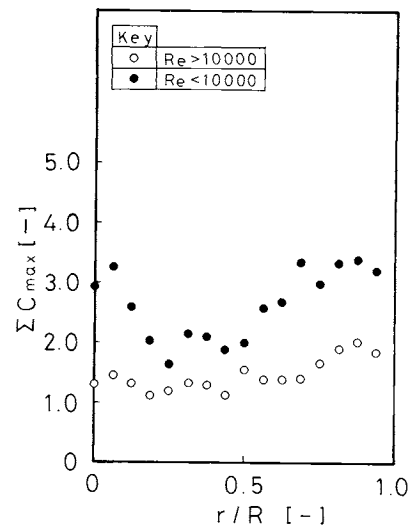

Fig. 9. Radial distribution of ΣC_{max}.

the lower-frequency eddy-group has some relation to the diffusion phenomena.

2) ΣC_{max} The summation of the height of peaks becomes an index which expresses the amount of time scale concerning the lower-frequency eddy-group. The averages of ΣC_{max} at each radial position for the two Reynolds number groups are calculated in the same way as in the case of $\bar{W}$, and the results are shown in **Fig. 9**. At any radial position, ΣC_{max} is larger at the low Reynolds number group than that at the high Reynolds number group. This confirms the prediction that the time-scale of the lower-frequency eddy-group for the low Reynolds number group is larger than that for the high Reynolds number group.

In the following section, some information about the lower-frequency eddy-groups is obtained from the patterns directly by observation and the results are compared with those obtained in this section.

3.2 Direct method

Figure 10(a) and (b) are contour line maps of the dimensionless velocity fluctuation (u/u'). The contour lines are drawn at intervals of dimensionless velocity fluctuation of 0.25, and each numerical value in these figures expresses the value of the line. The regions occupied by the lower-frequency eddy-groups are determined with the eye by the following steps.

1. Find a contour line which is closed and is extended over more than two radial positions.
2. Outermost contour line is taken to be the boundary of the region.

The shaded portion in Fig. 10(a) is an example of such a region.

All regions that meet these criteria are taken out of the maps, and their dimensionless radial sizes (L) are measured by using pipe inner radius. The determination of the intervals of the contour lines is important, because the size of the eddy-group described

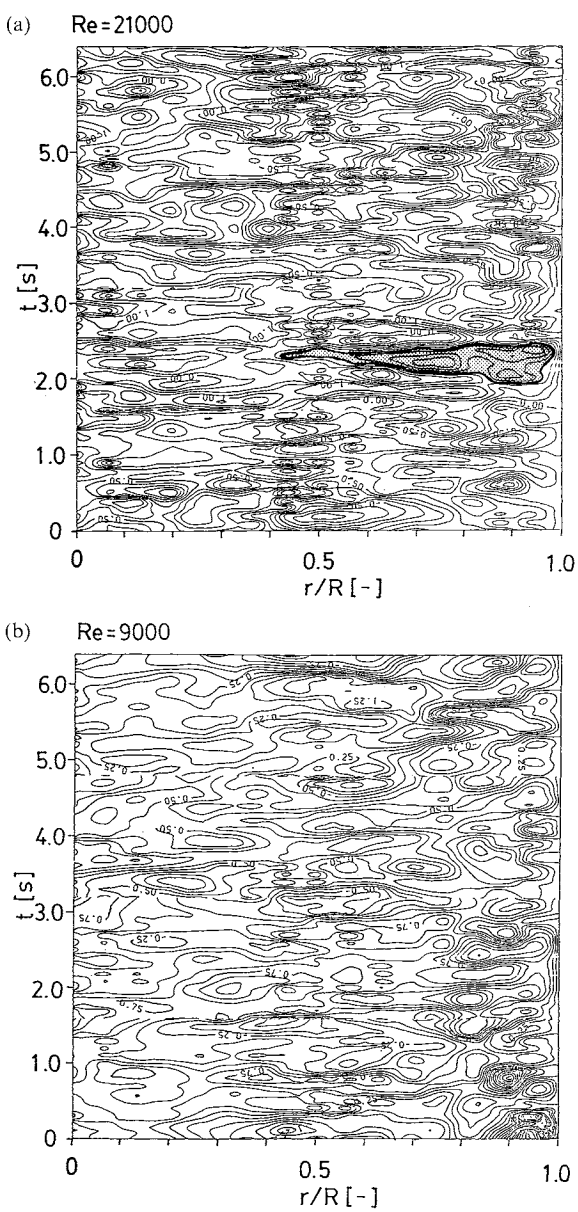

Fig. 10. Contour line map of dimensionless velocity fluctuation. (a) $Re=21000$; (b) $Re=9000$.

above depends greatly upon the intervals. If the contour lines are drawn more densely, more regions where contour lines are closed appear in the maps. But, in the newly appearing regions, the values of the dimensionless velocity fluctuations are predicted to be larger or smaller by 0.1 or 0.2 at most than those in the surrounding regions and the velocity fluctuations in these regions are predicted to contribute hardly at all to energy-spectra. Therefore, it is not necessary to draw contour lines more densely. **Figure 11**(a) and (b) show examples of the radial distributions of L. The solid curve in the figures shows the radial distribution of $\bar{W}$ obtained in the previous section. One-half of the value of $\bar{W}$ at each radial position is taken as the representative threshold that divides the distributions into the two groups as a trial. One group, which has a larger radial space-scale than the threshold, is expressed with white keys, and the other group, which has a smaller radial space-scale than the threshold, is expressed with black keys in these figures. There is little difference between the radial distribution of white keys and the solid curve of $\bar{W}$ at any Reynolds number, and the distribution of black keys is almost flat over the cross section of the pipe. From the results described above, it can be seen that the capacity of mixing at each radial position does not depend on the smaller eddy but on the larger one. This prediction is derived from the similarity between the distribution of eddy diffusivity and that of the scale of the larger eddy.

Because most of the smaller eddies are contained in a larger one, it is very difficult to find the smaller eddy statistically by the old statistical method. In this section, it is made clear that both the smaller and the larger eddies can be found directly from the contour line maps of the velocity fluctuation.

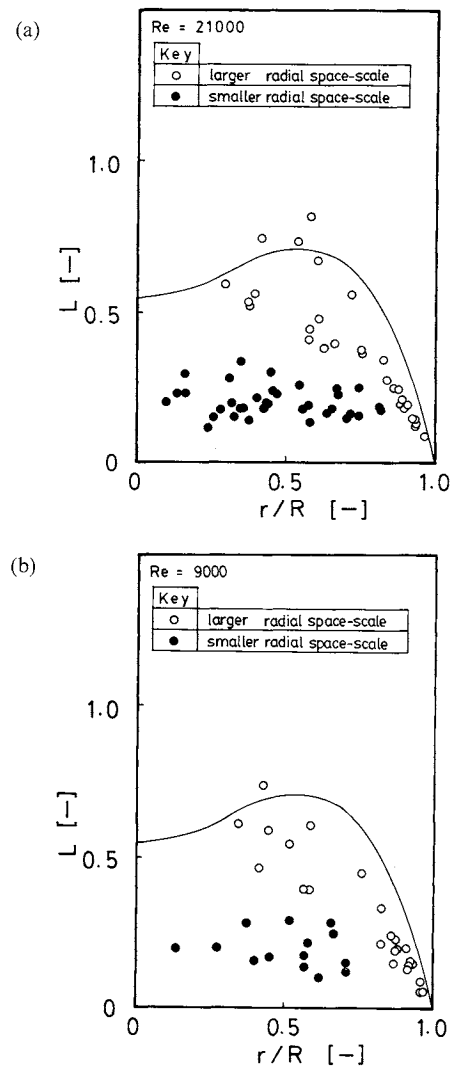

Fig. 11. Radial distribution of L. (a) $Re=21000$; (b) $Re=9000$.

Conclusion

Contour line maps of velocity and velocity fluctuation in turbulent pipe flow are drawn in order to reveal the turbulent structure. The shape and the scale of the lower-frequency eddy-group are shown clearly by these maps. By analyzing the maps with the statistical method, two indices concerning the scale of the lower-frequency eddy-group are defined. One of them corresponds to the time-scale, the other to the radial space-scale. On the other hand, by analyzing the maps by the direct method, the radial space-scale of the lower-frequency eddy-group is determined with the eye. From the radial distribution of this scale, it is found that there is a small eddy which has constant scale regardless of radial position in the lower-frequency eddy-groups from the view-point of the radial space-scale.

By using the contour line maps, new information about the radial space-scale of the lower-frequency eddy-group is obtained, and it is expected that more detailed consideration of the maps will introduce new information about the turbulent structure.

Nomenclature

C	=	correlation coefficient for one-dimensional arrangement of data	[—]
d	=	distance between two data in one-dimensional arrangement of data	[—]
L	=	radial space-scale of eddy on contour line map	[—]
R	=	pipe inner radius	[m]
Re	=	Reynolds number	[—]
r	=	radius	[m]
t	=	time	[s]
U	=	axial velocity	[m/s]
u	=	fluctuating part of axial velocity	[m/s]
u'	=	turbulent intensity	[m/s]
W	=	width of a peak in correlation curve	[—]

Literature Cited

1) Hinze, J. O.: "Turbulence," 2nd Edition, p. 730 (1975).

2) Ito, S. and K. Ogawa: *J. Chem. Eng. Japan*, **6**, 231 (1973).
3) Ito, S., K. Ogawa and T. Yuhara: *Kagaku Kōgaku*, **37**, 698 (1973).
4) Ogawa, K., C. Kuroda and S. Yoshikawa: *J. Chem. Eng. Japan*, **18**, 544 (1985).
5) Ogawa, K., C. Kuroda and S. Yoshikawa: *J. Chem. Eng. Japan*, **19**, 345 (1986).

FORMATION OF NICKEL CONCENTRATION PROFILE IN NICKEL/ALUMINA CATALYST DURING POST-IMPREGNATION DRYING

YOSHIMITSU UEMURA, YASUO HATATE AND ATSUSHI IKARI
Department of Chemical Engineering, Kagoshima University, Kagoshima 890

Key Words: Mass Transfer, Nickel Concentration Profile, Nickel Alumina Catalyst, Impregnation, Electron Probe Microanalysis, Solute Migration Model

Nickel concentration profiles were studied for impregnated nickel/alumina catalysts prepared by impregnating two types of spherical aluminas with nickel (II) chloride aqueous solution and applying a wide range of post-impregnation drying conditions. Migration of nickel (II) ion towards the outer surface of alumina occurred during post-impregnation drying. The fraction of migrated nickel (II) ion increased with increase of the constant drying rate, and was held at a constant value, 0.5, at values of the constant drying rate larger than 2×10^{-4} kg·m^{-2}·s^{-1}.

A model of solute migration during post-impregnation drying, combining solution movement by a capillary force with solute diffusion, was proposed. The observed nickel concentration profiles of the nickel/alumina catalysts showed good agreement with the results calculated by the model over the whole range of drying conditions.

Introduction

Impregnation is one of the most important industrial methods of preparing supported catalysts. Since Maatman[10,11] introduced the concept of movement of an active material precursor within supports during impregnation, many studies[5,6,9,16] of the phenomena have been reported. Recently, the majority[1,7,14] of such studies are concerned with control of the profile of an active material precursor. It seems that the techniques to obtain a desired concentration profile of an active material precursor during impregnation are established to some extent. However, the profile formed during impregnation may be destroyed by post-impregnation drying, which causes migration of an active material precursor toward the outer surface of supports, i.e., surface segregation.[4,7,15]

Kotter *et al.*[8] reported that addition of hydroxyethylcellulose to the impregnating solution depressed the surface segregation. However, the decrease of penetration rate of the impregnating solutions due to viscosity increase makes the technique a restricted one. To solve such a problem, quantitative investigation of the surface segregation of an active material precursor is preferable, but no model for interpreting that phenomenon quantitatively has been found.

In the present study, the effects of the post-impregnation drying conditions on the nickel concentration profiles of impregnated nickel/alumina catalysts were investigated by impregnating two types of spherical aluminas with nickel (II) chloride aqueous solution and applying a wide range of drying conditions. Furthermore, a model of solute migration during post-impregnation drying is proposed to describe the nickel concentration profiles.

1. Experimental

1.1 Preparation of catalysts

Eighteen kinds of impregnated nickel/alumina catalysts were prepared by using two types of aluminas (JRC-ALO-1 and JRC-ALO-3 supplied by Catalysis Society of Japan) and applying nine kinds of post-impregnation drying conditions. The typical properties of the supports and the preparation conditions are presented in **Table 1**.

1) Impregnation Spherical aluminas of average diameter about 3 mm were impregnated with nickel

Received June 30, 1986. Correspondence concerning this article should be addressed to Y. Uemura.